

## VARIATION OF THE HEIGHT OF CENTRELINE OF A HELIOSTAT AND INFLUENCE ON THE WIND LOADING

Poulain P.E., Craig K.J.\* and Meyer J.P.

\*Author for correspondence

Department of Mechanical and Aeronautical Engineering,

University of Pretoria, Pretoria, 0002, South Africa,

E-mail: [ken.craig@up.ac.za](mailto:ken.craig@up.ac.za)

### ABSTRACT

Mostly located in desert areas, heliostat fields are subjected to various wind conditions. An ANSYS Fluent CFD model of a single heliostat in some worst-case positions is produced using numerical simulations with the realizable k- $\epsilon$  model. The intent of this paper is to show the possible effect that the clearance gap has on the force and moment coefficients of the heliostat. The incoming flow modeled is an ABL profile that has already been generated in a wind tunnel. For a wind angle of  $0^\circ$  and heliostat elevation angles of  $90^\circ$  and  $30^\circ$ , the HCL is varied and the force and moment coefficients are computed. It is shown that the coefficients are sensitive to the clearance gap. More specifically, there is a compromise between lift and drag, and a specific HCL is beneficial to minimize the hinge moment.

### INTRODUCTION

The heliostats field can represent about 50% of the total investment needed to build a solar tower power plant [1]. Because of this, finding ways to increase the optical efficiency of the field and to build heliostats with cheaper or less material is a key point regarding the profitability of the power plant. However, the important factors in the design of a heliostat (manufacturing, sizing and wind loading) comprise numerous and strongly inter-related variables [2].

An important step in structural design is gathering information about the loading that a facility will undergo. So far, the wind tunnel tests are the preferred way to evaluate the wind loading experienced by heliostats models. Computational Fluid Dynamics (CFD) is becoming more and more popular as it enables to decrease the amount of costly wind tunnel tests.

One of its best advantages is that changing the shape or the dimensions of the model tested is convenient and several options can be explored before undertaking wind tunnel tests.

Several experimental and CFD studies have investigated different possibilities to decrease the wind loading to which heliostats are exposed to. The presence of a perimeter fence [3] shows a significant drop in the loads undergone by the outer heliostats. Concerning the aspect ratio, a trade-off driven by the

costs of the different drives used to rotate the heliostats is to be found, with a higher aspect ratio presenting a lower drag force but a higher azimuthal moment and vice versa [4]. Recent research provides a CFD model that minimizes the contribution of both the hinge and azimuthal moments with an aspect ratio of 1.1 [5]. The current study uses an aspect ratio of 1 that is similar to that used in [3].

### NOMENCLATURE

$A$	[m <sup>2</sup> ]	Reflector area
$C_F$	[-]	Force coefficient
$C_M$	[-]	Moment coefficient
$C_\mu$	[-]	Turbulence models constant
$F$	[N]	Wind induced force
$I_u$	[%]	Streamwise turbulence intensity
$k$	[m <sup>2</sup> /s <sup>2</sup> ]	Turbulent kinetic energy
$L$	[m]	Characteristic length of heliostat
$M$	[Nm]	Wind induced moment
$U_{ABL}^*$	[m/s]	Friction velocity of the atmospheric boundary layer
$x, y, z$	[m]	Cartesian axis directions
$z_0$	[m]	Aerodynamic roughness length

#### Special characters

$\alpha$	[°]	Heliostat elevation angle
$\beta$	[°]	Wind azimuthal angle
$\epsilon$	[m <sup>2</sup> /s <sup>3</sup> ]	Turbulence dissipation rate
$\kappa$	[-]	von Karman constant
$\rho$	[kg/m <sup>3</sup> ]	air density

#### Subscripts

$ref$	Reference value
$x, y, z$	In the direction of x, y or z

#### Abbreviations

$ABL$	Atmospheric boundary layer
$CFD$	Computational fluid dynamics
$HCL$	Height of the centreline

Because of expensive wind tunnel tests, CFD has become a useful tool in research and development. E.g., a numerical study focused on the influence of the gap size between the panels of a single heliostat [6]. A numerical model of a heliostat under different operating conditions argued that

satisfactory results can be obtained when compared to wind tunnel experimental data [7]. An ABL inlet condition has been simulated to obtain physically accurate results.

The current paper investigates the use of ANSYS Fluent to study the effect of the placement of the centre of the heliostat, or HCL, as a parameter that would reduce the drag in more upright positions, but also reduce the hinge moment at operational heliostat angles for higher sun positions. After a description of the model geometry, a validation study is presented that uses data of Peterka et al. [3]. Settings from the validation study (especially regarding the inlet profile for velocity and turbulence intensity) are then applied to a parametric study in which the HCL is varied for two heliostat elevations. The paper concludes with suggestions for reduction in the force and moment coefficients.

## VALIDATION

### Geometry

For validation, we aim to replicate the single square heliostat wind tunnel test of Peterka et al. [3] with an ANSYS Fluent v15.0 CFD model, using the same heliostat model and a fairly similar inlet mean velocity profile. The same coordinate system has also been employed (Figure 1).

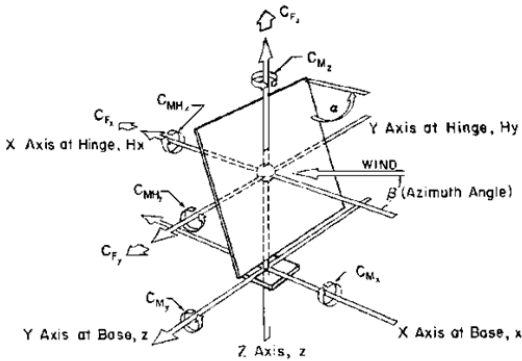


Figure 1 Coordinate system [3]

In ABL profiles, the near-ground region has low mean velocities but high turbulence intensities. This can be a source of deflections for a heliostat as the clearance gap is generally quite small (e. g. 10 mm, model scale, for Peterka et al. [3]). Consequently, a study of the clearance gap could provide indications about a favourable range of clearance gaps as well as ranges to be avoided.

### Inlet profiles

The mean velocity profile has been extracted in [3] from the wind tunnel data and interpolated using a logarithmic law (equation (1)). The least squares method gives an optimum of 0.07 mm for the aerodynamic roughness length,  $z_0$ .

$$U(z) = U_{ref} \frac{\ln\left(\frac{z}{z_0}\right)}{\ln\left(\frac{z_{ref}}{z_0}\right)} \quad (1)$$

Note that the reference height is 1.016 m (model scale) but the value for the reference mean velocity at this height is not mentioned in the report [3]. However, considering the non-

dimensional quantity  $\frac{U(z)}{U_{ref}}$ , the least squares method can be applied and  $U_{ref}$  can be calculated afterwards (11.9 m/s) by using the known velocity at the HCL.

In order to obtain a fully developed ABL inlet profile, equation (2-4) have to be satisfied. The friction velocity,  $U_{ABL}^*$ , is calculated from the reference values.

$$U(z) = \frac{U_{ABL}^*}{\kappa} \ln\left(\frac{z}{z_0}\right), k = \frac{U_{ABL}^{*2}}{\sqrt{C_\mu}} \text{ and } \varepsilon(z) = \frac{U_{ABL}^{*3}}{\kappa z} \quad (2-4)$$

Then, with the assumption of isotropic turbulence, the turbulence intensity profile can be determined using equation (5). This should result in a horizontal homogenous inlet profile.

$$I_u(z) = \frac{\sqrt{\frac{2}{3}}k}{U(z)} \quad (5)$$

In Figures 2a and 2b, one can see the mean velocity and turbulence intensity profiles used. The mean velocity profile matches with the one generated by Peterka et al. [3]. The turbulence profile matches in shape but is significantly under-predicted. This is one important limitation of the model since the turbulence intensity has a high influence on the wind loading. Although this would result in a lower mean velocity, one can increase the turbulence intensity by increasing  $z_0$ . Trying to match the turbulence profile through the turbulent kinetic energy would result in changing the value of the turbulence model's empirical constant  $C_\mu$ . At the model HCL, the turbulence intensity is 8.4% compared to 18% measured during the wind tunnel test.

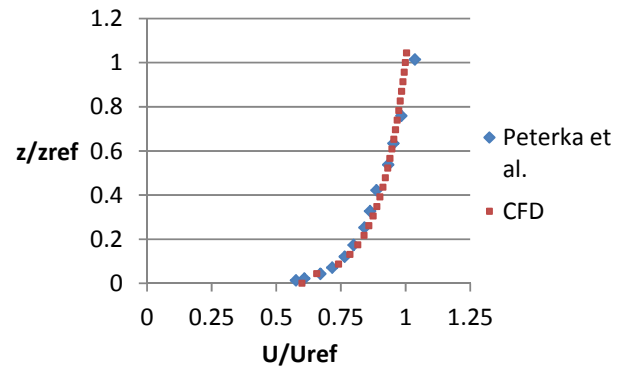


Figure 2a Mean velocity profiles

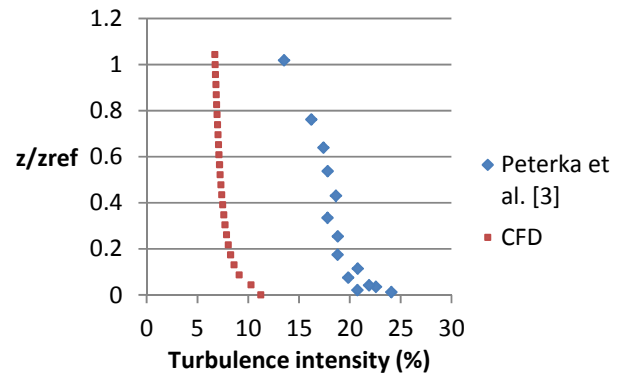
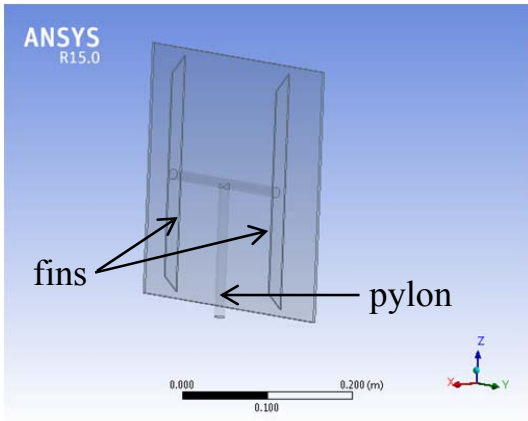


Figure 2b Turbulence profiles

**Computational domain**

As displayed in Figure 3a, the heliostat model is nearly the same as the one in [3] with an aspect ratio of 1 for a characteristic length of 297 mm. The aspect ratio remains constant throughout the study. The thickness of the fins supporting the reflector was set to 2 mm. The computational domain (Figure 4) represents the test section. The cross sectional area is 2x2 m<sup>2</sup> and the length of the channel is 3.5 m.

It is crucial to have a sufficient space before the model otherwise the latter has a blockage effect on the incident flow and it leads to over-predicted values. For the simulations, the inlet profiles are generated 1.5 m before the model. There are two zones of influence: the local volume surrounding the heliostat model and the wake area behind the model stretching to the outlet of the domain. Around these two zones, the domain has been divided into three parts to allow for meshing using stretching in order to preserve accuracy with fewer computational cells.



**Figure 3a** Heliostat model

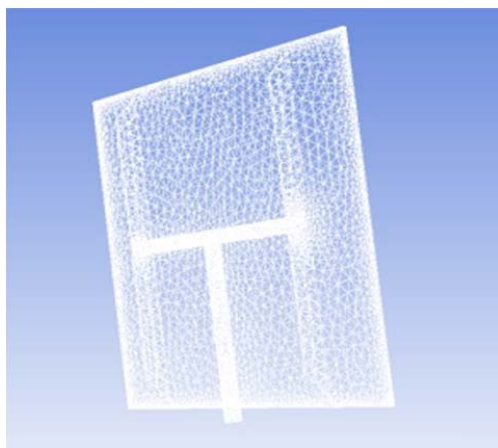


**Figure 3b** Heliostat mesh

The heliostat model is enclosed in a box meshed with tetrahedrons (Figure 3b), more convenient for round shapes and sharp edges. The rest of the domain is meshed with hexahedrons to reduce the computational time (Figure 4). The borders of the box containing the heliostat model are treated with mesh interfaces whilst the mesh is conformal elsewhere.

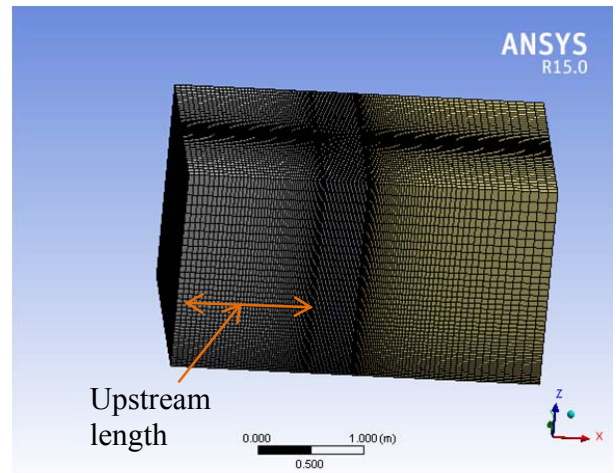


**Figure 4** Computational domain

It is important to verify that the incident profile seen by the heliostat is the same as the one generated at the inlet. As respectively shown on Figure 5 and 6, both the mean velocity and turbulence intensity profiles present a similar shape and order in between the inlet and the heliostat. The profiles have been visualized at the inlet, 0.5, 1 and 1.5 m away from the inlet, at the centre of the channel. Although the turbulence seems to dissipate in the viscous sublayer, the slight decay is acceptable and we can consider the ABL profile to be horizontally homogenous.

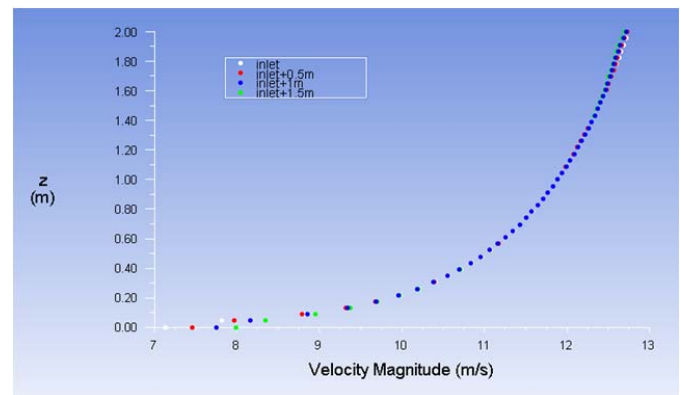


**Figure 5** Mean velocity profile at x=0 (inlet), 0.5, 1 and 1.5 m

**Boundary conditions**

The fluid is defined as incompressible air. The side and top walls satisfy a zero shear-stress condition. This has the effect to force the flow to be parallel to these walls. The ground and the heliostat have no-slip wall conditions. The exit of the test section is set as a pressure outlet. The velocity and turbulence intensity profiles are generated by reading a User-Defined Function (UDF) containing equations (2-4) and (5). The mean velocity speed at the HCL is  $U_{HCL} = 9.6$  m/s.

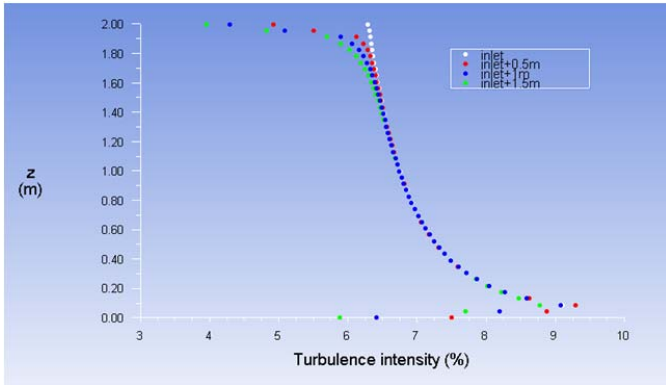


**Figure 6** Turbulence intensity profile at  $x=0$  (inlet), 0.5, 1 and 1.5 m

All the simulations have been run with the realizable  $k-\epsilon$  turbulence model with enhanced wall treatment to simulate fully turbulent flow.

## VARIATION OF HCL

### HCL in original position

Initially, the HCL is varied for a heliostat in a vertical position with the wind impinging on the panel perpendicularly. This is the maximum drag case. Then, the elevation angle is set to  $30^\circ$ , with the azimuth angle remaining at  $0^\circ$ . This latter position is the worst case for both the lift force and hinge moment coefficients.

During the simulations, the scaled residuals and all the force and moment coefficients (equation (6)) are monitored to ensure that convergence is reached. Note that  $C_{M_x}$  and  $C_{M_y}$  are based on the moments occurring at the hinge and not the pylon base and  $U_{HCL}$  has to be recalculated for every change in the HCL.

$$C_{F_{x,y,z}} = \frac{F}{\frac{1}{2}\rho U_{HCL}^2 A}, \quad C_{M_{x,y,z}} = \frac{M}{\frac{1}{2}\rho U_{HCL}^2 A L} \quad (6)$$

Several simulations presenting the inlet up to 3 m before the model have been run. Only small differences were noted when the inlet was set to 1.5 m before the model (5 times the model characteristic length) and this setup has been favoured, resulting in a lower computational cost.

The coefficients are compared against the wind tunnel data given in [3] and presented in Table 1. The result given by the CFD for  $C_{F_x}$  is then coherent. This is seen in Figure 7 presenting the results of several wind tunnel tests from literature. The CFD data point being drawn with the two blue lines corresponds to the current study. This value seems to match with the uniform flow study of Bearman [8] which showed that a low turbulence intensity ABL profile tends to give similar results as a uniform flow profile. Peterka et al. [3] obtained a drag coefficient above 2 due to the high turbulence intensity (18%) at the heliostat HCL (highest data point in Figure 7).

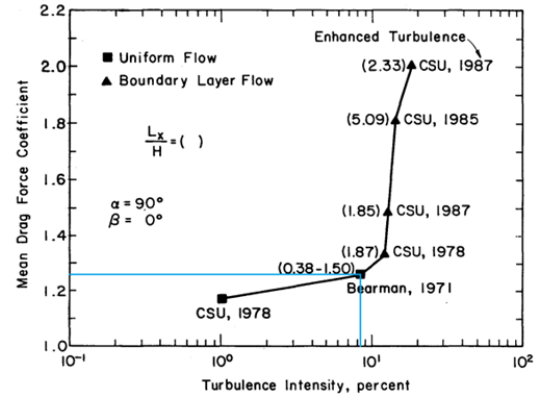


**Figure 7** Drag coefficient measured for the case  $\alpha = 90^\circ$  and  $\beta = 0^\circ$  in several studies [3]

Except for  $C_{F_x}$  and  $C_{M_y}$ , all the coefficients are close to 0 in the CFD results (Table 1). This is consistent with the symmetry of the model. In the experimental data, this is surprisingly not the situation when looking at the values for  $C_{F_y}$ ,  $C_{F_z}$  and  $C_{M_z}$ . One explanation could be the presence, upstream of the model, of relatively high cubes on the ground mimicking its roughness. The plate may however experience a slight hinge moment due to the three-dimensional shape of the ABL profile.

**Table 1** Force and moment coefficients for a wind angle of  $0^\circ$  and an elevation angle of  $90^\circ$

$\alpha = 90^\circ$ $\beta = 0^\circ$	$C_{F_x}$	$C_{F_y}$	$C_{F_z}$	$C_{M_x}$	$C_{M_y}$	$C_{M_z}$
Peterka et al.	2.093	0.084	-0.062	0.013	0.013	0.062
CFD (inlet 1,5 m)	1.327	-6.40e-05	-7.03e-04	-5.91e-05	0.0243	5.01e-05
CFD (inlet 3 m)	1.337	3.48e-04	-6.63e-04	-4.09e-05	0.0274	-1.67e-04

### Modification of the HCL

When the heliostat is in a higher position, it undergoes a more uniform turbulence intensity profile of a lower magnitude but the approach mean velocity is higher (Figure 2a and b). In Peterka et al.'s experiment [3], the height of the pylon is 158.5 mm and the clearance gap is 10 mm. As a first modification, these dimensions will be brought up and down by up to 5 mm. This will give a first trend as to whether the model should rather be lowered than lifted. Then, the reflector will be inclined with an elevation angle of  $30^\circ$  (for  $\beta = 0^\circ$ ), as mentioned earlier, and the same procedure will be followed with the same HCL mean velocity to be consistent with Peterka et al. [3] (still 9.6 m/s).

### Results for the HCL

Regarding the position  $\alpha = 90^\circ, \beta = 0^\circ$ , the drag coefficient increases with the HCL (Figure 8). Indeed, the heliostat seems to experience more drag when the approach mean velocity is higher and the turbulence intensity lower. On the other hand, the hinge moment coefficient,  $C_{M_y}$ , decreases when the HCL is

raised. This is expected when considering the turbulence intensity profile which becomes more uniform with an increase in height therefore inducing a smaller moment.

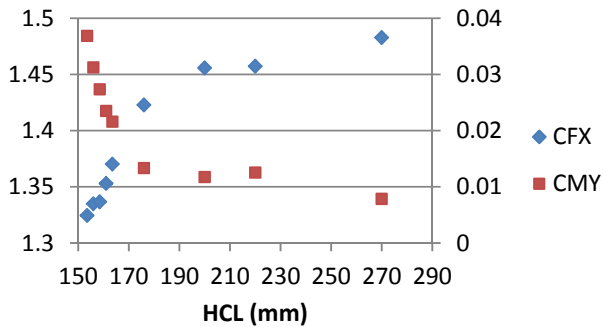


**Figure 8** Variation of  $C_{Fx}$  (left ordinates) and  $C_{My}$  (right ordinates) with different HCL for  $\alpha = 90^\circ$  and  $\beta = 0^\circ$

The drag force and the hinge moment have an opposite response when varying the HCL (Figure 8). It is possible to reduce stresses caused by  $C_{My}$ , but the drag would be increased. When comparing HCL=153.5 mm and HCL=163.5 mm, the drag coefficient raises by about 3% whilst the hinge moment coefficient drops by more than 40%. The other force and moment coefficients are not plotted, as they do not present any particular trend, because of their magnitude being very small.

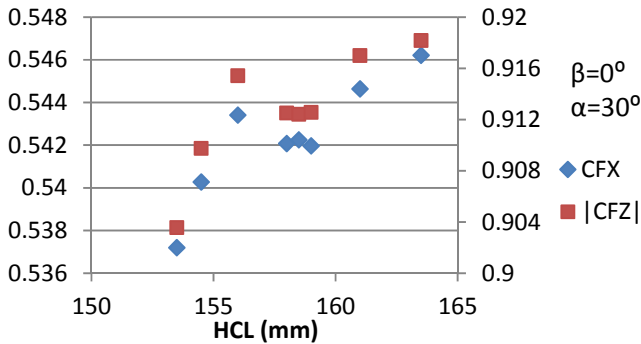


**Figure 9** Variation of  $C_{Fx}$  (left ordinates) and  $|C_{Fz}|$  (right ordinates) with different HCL for  $\alpha = 30^\circ$  and  $\beta = 0^\circ$

As for the position  $\alpha = 30^\circ$  and  $\beta = 0^\circ$ , Figure 9 and 10 globally show that the closer to the ground the heliostat is, the lower are the magnitudes of  $C_{Fx}$ ,  $C_{My}$  and  $C_{Fz}$ . One can see from the local minimum at HCL=158.5 mm that this HCL value may provide a good compromise for these coefficients if a larger ground clearance is desired.

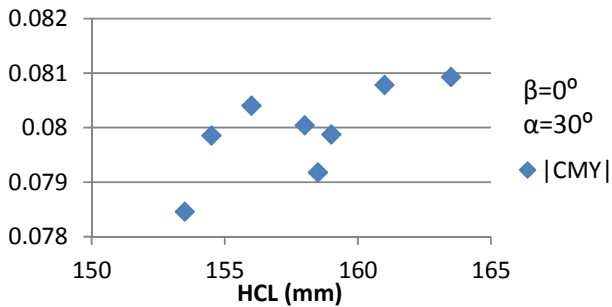


**Figure 10** Evolution of  $|C_{My}|$  with the HCL for  $\alpha = 30^\circ$  and  $\beta = 0^\circ$

### Visualization of the flow

In this subsection, we present different views of the flow field surrounding the heliostat and talk about their evolution with the HCL. As displayed in the following figures, the flow pattern is similar to other studies and presents several recirculation zones. In the wake area, two zones show a different behaviour in terms of mean velocity (Figure 11).

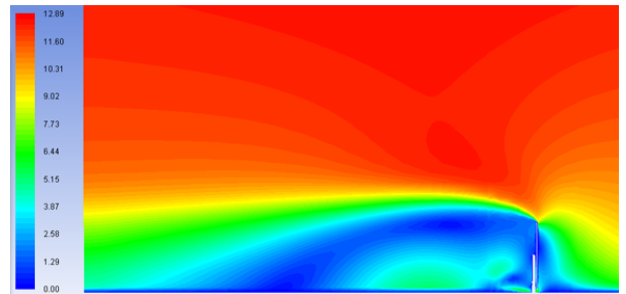


**Figure 11** Velocity (m/s) flow field in z-x plane around vertical heliostat, HCL=163.5 mm

The area above the HCL is exposed to low magnitudes with the air flowing streamwise whilst the region beneath experiences higher magnitude backflow. Below the reflector, the flow separation occurring due to the clearance gap is also visible and creates a smaller recirculation zone (Figure 12). The difference with an inclined heliostat is that the recirculation zones (z-x plane) are located before and after the pylon (Figure 13).

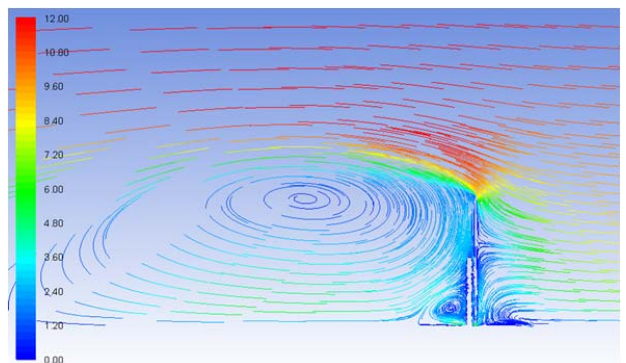


**Figure 12** Streamlines coloured by velocity magnitude (m/s) in z-x plane around vertical heliostat, HCL=153.5 mm

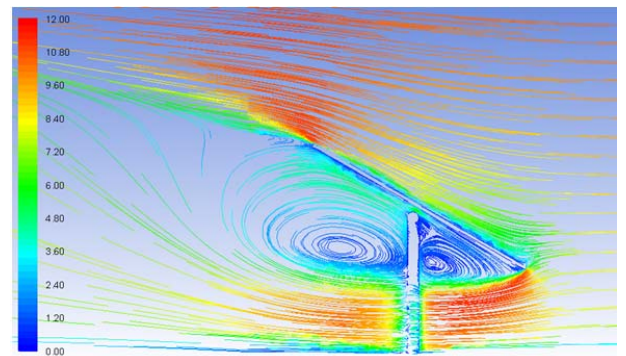


**Figure 13** Streamlines coloured by velocity magnitude (m/s) in z-x plane around inclined heliostat (b), HCL=153.5 mm

If we significantly increase the HCL, a slightly different pattern occurs. In Figure 14, the clearance gap is wide enough to allow a part of the flow to push through at higher velocities. The minor recirculation, seen before in Figure 12, is now much bigger and the two vortices are nearly of the same size. This can explain the lower hinge moment for a higher HCL as the upper and lower parts of the reflector are more in balance. At the same time, the drag is increased, and the heliostat experiences a larger suction effect all around the torque tube.

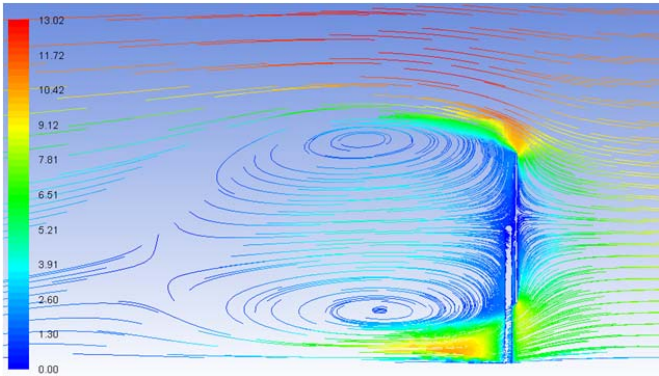


**Figure 14** Streamlines coloured by velocity magnitude (m/s) in z-x plane around vertical heliostat, HCL=270 mm

As displayed in Figure 15, the wake visualized in a top view plane presents two long vortices originated by the flow separation at the vertical edges of the heliostat.

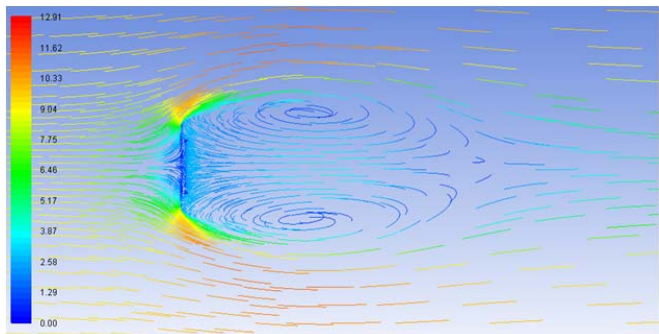


**Figure 15** Streamlines coloured by velocity magnitude (m/s) in x-y plane for a vertical heliostat, HCL=153.5 mm

## CONCLUSIONS

After a grid and domain dependency verification, a comparison with literature indicated that the CFD model gives lower values for the drag force coefficient. This is a result of the under-prediction of the inlet turbulence intensity profile (18% versus 8% in this study). However, this level of inlet turbulence did result in a meaningful variation of force and moment coefficients with the variation of the heliostat centreline position.

Regarding the maximum lift force and hinge moment orientation ( $\alpha = 30^\circ$ ,  $\beta = 0^\circ$ ), a lower HCL results in lower force and moment coefficients as expected, but a local minimum in all the coefficients was observed at an HCL of

about 158 mm. Interestingly, this local minimum HCL corresponds closely to the value used by Peterka et al.

Concerning the maximum drag force position (vertical heliostat), one can decrease the hinge moment by increasing the HCL. Starting from a clearance gap of 5 mm, the hinge moment drops by more than 40% when the clearance gap is brought up to 15 mm. The drag force correspondingly increases by only 3%. This hinge moment result could find application if the heliostats stow position is vertical.

It was not possible to match the wind tunnel test results. This is due to the mismatching turbulence profile. If the turbulence intensity and the mean velocity were to be decoupled, the condition of horizontal homogeneity would not be achieved and one could obtain non-physical results.

In this study, the focus was on the ground clearance through variation of the HCL. For an optimum clearance gap, one can find an aspect ratio that minimize the force and moment coefficients.

## ACKNOWLEDGEMENTS

The authors would like to acknowledge the support from the University of Pretoria (South Africa) and the South African National Research Foundation (DST-NRF Solar Spoke).

## REFERENCES

- [1] Pfahl A., Survey of heliostat concepts for cost reduction, *Journal of Solar Energy Engineering*, Vol. 136 (1), 2013
- [2] Coventry J. and Pye J., Heliostat cost reduction – where to now?, *Proceedings of the SolarPACES 2013 Conference*
- [3] Peterka J. A., Tan Z., Bienkiewicz B. and Cermak J.E., Mean and peak wind load reduction on heliostats, Technical Report for Solar Energy Institute, September 1987
- [4] Pfahl A., Buselmeier M. and Zschke M., Wind loads on heliostats and photovoltaic trackers of various aspect ratios, *Solar Energy*, Vol. 85, 2011, pp. 2185-2201.
- [5] Marais M.D., Craig K.J. and Meyer J.P., Computational flow optimization of heliostat aspect ratio for wind direction and elevation angle, *Proceedings of the SolarPACES 2015 Conference*
- [6] Wu Z. and Wang Z., Numerical study of wind load on heliostat, *Progress in Computational Fluid Dynamics, an International Journal*, Vol. 8, Nos 7/8, 2008, pp. 503-509
- [7] Wang Y. and Zhengnong L., Research on Numerical Simulation of Heliostat's Surface Wind Pressure, *Key Engineering Materials*, Vol. 517, 2012, pp 809-816
- [8] Bearman P.W., An investigation of the forces on flat plates normal to a turbulent flow, *Journal of Fluid Mechanics*, Vol. 46, part 1, 1971, pp. 177-198